CAST AND MACHINED POROUS CARBON STRUCTURES MADE FROM WHEY

Raúl Llamas-Unzueta1, Luis A. Ramírez-Montoya1, Jaime Viña2, Antonio Argüelles3, Miguel A. Montes-Morán1 y J. Angel Menéndez1

1 Instituto de Ciencia y Tecnología del Carbono - CSIC. Calle Francisco Pintado Fe, 26 - 33011 Oviedo (Spain).

2 Universidad de Oviedo. Dpto. de Ciencia de Materiales e Ingeniería Metalúrgica. C/ Independencia 13, s/n - 33004 Oviedo (Spain).

3 Universidad de Oviedo. Dpto. de Construcción e Ingeniería de Fabricación. Calle San Francisco, 3 - 33003 Oviedo (Spain).

Received: 08/jan/2021 • Reviewing: 13/jan/2021 • Accepted: 25/mar/2021 - DOI: https://doi.org/10.6036/10054

To cite this article:

LLAMAS-UNZUETA, Raúl; RÁMIREZ-MONTOYA, Luis; VIÑA, Jaime; ARGÜELLES, Antonio, MONTES-MORÁNA, Miguek; MÉNENDEZ, J. Angel. MOLDABLE AND MACHINABLE POROUS CARBON STRUCTURES OBTAINED FROM WHEY. DYNA. July 2021, vol. 96, no. 4, p. 422-428. DOI: https://doi.org/10.6036/10054

ABSTRACT:

A new porous carbon structures made by sintering whey powder in a mold at 150ºC and subsequent carbonization and/or activation are described. These porous carbon structures represent a step beyond simple activated carbon monoliths, as they can take the shape of any mold and machined if necessary. These carbon materials have a porosity that can reach up 70%, made up of a system of hierarchical and interconnected pores, which gives them a high permeability. Furthermore, they have a much higher mechanical strength than other porous carbon monoliths.

Key Words: carbon structures, monoliths, porous carbon, activated carbon, machining, sintering, whey, whey powder.

1. - INTRODUCTION

In recent years, much progress has been made in the control of the porous texture and the surface chemistry of porous carbons (activated carbons), being able, with some precision, to manufacture carbons with a porous texture and a surface chemistry adapted to a particular application. [1]. However, while this happens at the nanometric level; at the macroscopic level, the shape and geometry of porous carbons is almost exclusively limited to powders, grains, pellets, fabrics and monoliths with very simple geometries (Fig. 1).

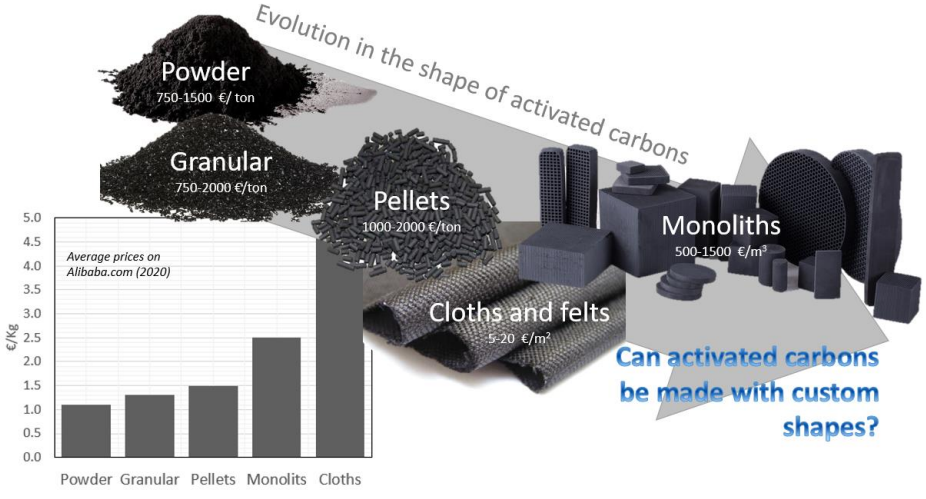

Fig. 1. Different shapes of activated carbon and their average price (in 2020).

It should be noted that as "design" is added to activated carbons, their price increases considerably; in such a way that the structures with "more design", like fabrics or monoliths, are not sold by weight but by area or volume, respectively (Fig.1). However, compared to other materials, porous carbons are very limited in making them with complex structures or sophisticated shapes and designs that allow new applications or improve existing ones.

Currently, the most widely used raw materials for the production of activated carbon are carbon and coconut shell [2]. However, these precursors are conditioned to extractive activities with high environmental impact and decreasing availability, in the case of coal; and seasonality, climatic variability and external producing countries, in the case of coconut shell. In addition, the growing demand for activated carbon makes it necessary to find new economic, renewable and environmentally friendly precursors.

On the other hand, although whey is a natural and 100% sustainable product, it is also a very difficult residue to eliminate due to its high biochemical oxygen demand (BOD/COD) and water content (ca. 90 wt%). Therefore, with more than 80 million tons/year of surplus whey in the world [3], there is a great need to find new uses for all these leftovers.

This work aims to provide a partial solution to these two problems using dehydrated whey powders for the manufacture of porous carbon structures by sintering them in a mold at 150ºC and subsequent carbonization and/or activation.

2. - MATERIALS AND METHODS

2.1. Whey for obtaining porous carbon structures

Dehydrated whey powders (W) were supplied by the Spanish dairy company Central Lechera Asturiana (CAPSA-FOOD). This whey is obtained by spray drying in drying towers with a production rate of 2 tons/hour, a moisture content of 3% approximately, and particle sizes between 10 and 200 µm, although predominant sizes are those about 20 µm. Whey powders were used in such way like were received, with no further treatments or handling. Main characteristics of whey are listed on Table 1. Macroscopic and microscopic morphology can be observed at the pictures shown in Fig.1.

Table 1. Composition, elemental analysis and pH of powdered whey.

Main components (wt%)		Elemental Analysis[b] (wt%)	
Carbohydrate (Lactose)	78.4	C[c]	40.7
Proteins	12.7	H[c]	6.3
Fats	1.8	N[c]	2.3
Ashes	4.4	O[c]	46.1
Moisture	2.7	S[c]	0.2
pH_{sat}[f]	5.1	Na[d]	0.3
[a] Producer specifications		K[d]	1.2
[b] Dry basis		Mg[d]	0.1
[c] Organic elemental analysis (CHNSO)		Ca[d]	0.4
[d] ICP-MS;		P[d]	0.6
[e] Cl, ISE		Cl[e]	0.2
[f] pH of a saturated solution of whey			

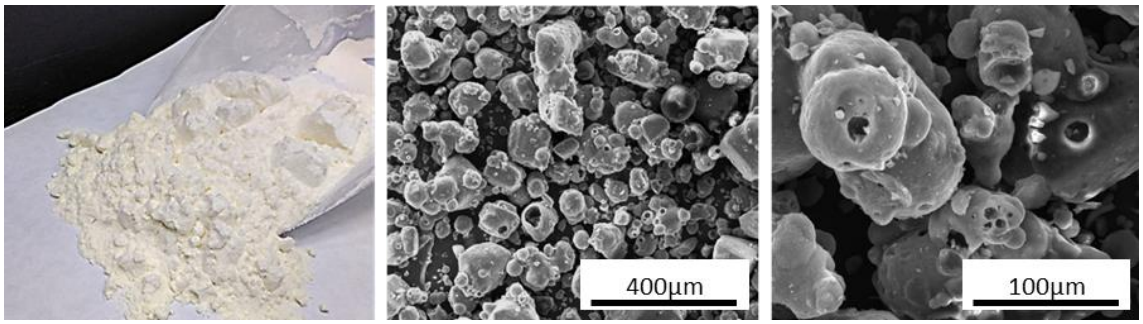

Fig. 2. Physical appearance (left) and SEM photomicrographs of whey powder.

2.2. Manufacture of the porous carbon structures

The manufacture of the structures begins with the filling of a mold, which can be made of any material suitable of containing the whey powders and withstanding 150ºC without deforming. In this work, most of the molds used were made of silicone or steel. No pressure

was applied to the powders after molding. Compaction of powders by pressure is not necessary. Once the mold is filled, whey powders are subjected to a heat treatment at 150 ° C for approximately one hour. After this time, the powders are sticked together, in a "pseudo-sintering" process, forming a piece that adopts the shape of the mold. During this stage there is a small (<0.5%) contraction of the resulting piece comparing to the mold, which makes demolding much easier. This pseudo-sintering process is similar to sintering, although it does not require external pressure, since the particles are joined to each other only by the effect of temperature, giving as a result a piece with sufficient consistency and suitable to be handled without difficulty. This step can be carried out both in an air atmosphere and in an inert one with no differences observed in the resulting materials.

Once the piece is demolded, it is carbonized in a tubular furnace under inert atmosphere, using 100 mL/min of N^2 as inert gas. Heating rate is 10ºC/min until final temperature, which corresponds to 850ºC for those structures named CW850. In order to increase micro porosity of resulting materials, the structures named AW850/1.5 are heated the same way than previously mentioned, but once the final temperature of 850ºC is reached, they are subjected to a flow of 50 mL/min of CO^2 for 90 min. At the end of the activation process, the pieces are cooled to room temperature under 100 mL/min N^2 flow.

Finally, some of the pieces were subjected to different machining processes to obtain the desired shape. This machining process is possible by the consistency and excellent mechanical properties exhibited by the resulting porous carbon structures.

A video of manufacturing and machining of these pieces can be seen at the supplementary material.

2.3. Characterization of the porous carbon structures

Immediate analysis (moisture, volatile matter and ashes) was carried out on a thermobalance Q5000 from TA Instruments. Moisture content was calculated from weight loss at 110°C under N_2 atmosphere. Volatile matter was determined by the difference between fixed carbon (solid matter that remains at 900ºC under N_2 atmosphere) and moisture. Ashes content is equivalent to the mass of residue after combustion at 900ºC in an air atmosphere.

Thermogravimetric analysis (TG) and (DTG) were performed on a Q5000 TA Instruments thermobalance under N2 and CO_2 atmosphere, using a heating rate of 10°C/min starting at room temperature up to 1000°C with a sample mass of 20 mg approximately.

Organic elemental analysis (CHNSO) was achieved in microanalyzers LECO CHNS-932 y LECO VTF-900.

Elemental analysis of other inorganic elements was carried out by ICP-MS in an Agilent 7700x apparatus, with exception of Cl determination, which was completed using an ion selective electrode (ISE).

The point of zero charge (pH_{pzc}) was calculated after grinding the porous carbon pieces below a particle size of 0.212 mm, and then preparing a suspension of 250 mg of this powder into 2 mL of distilled water. The suspension was kept closed and continuously stirred in a rotator mixer Intelli-Mixer RM-2M (40 rpm). The pH was measured daily as water was added. pHpzc value was obtained from the plateau of the pH variation curve.

Scanning Electron Micrographs (SEM) were taken in a Quanta FEG 650 device.

Adsorption N_2 isotherms from activated and carbonized samples were obtained using a volumetric adsorption system Micromeritics Tristar II at temperature of 196ºC. As a preliminary step, the samples were degassed by heating to 120ºC under vacuum conditions for 12 hours. The BET surface was determined using Brunauer-Emmett-Teller model and micropore volume was calculated from Dubinin-Radushkevich model. Real density of the materials (ρHe) was measured using a Micromeritics AccuPyc 1330 pycnometer, with He as pycnometric fluid. Hg intrusion was performed in a Micromeritics AutoPore IV porosimeter, reaching a maximum operating pressure up to 227 MPa. Apparent density (ρ_{Hg}) and pore size distribution (size range between 4nm to 100 µm) were both obtained from the intrusion curves. For both cases, samples were degassed at 120ºC during 12 hours before the analysis.

Intrinsic permeability (k) was measured passing an increasing He flow through the materials shaped as cylinders with 10 mm length and 10mm of diameter. Intrinsic permeability (k) is related to the gas volume flowing through the cross section of permeameter (v_L), the length of the cylinder (L), the viscosity of the gas (μ_{gas}), the final pressure (P_L) and the initial pressure (P_0), according to Darcy's equation:

$$k = 2v_L\mu_{gas}P_L/(P_0^2-P_L^2) \quad (1)$$

Flexural strength was measured from a 3 points flexural test using prismatic specimens. Test conditions were replicated from the standard test BS EN843-1: 2006 for advanced ceramics techniques. An apparatus MTS Systems Corporation model SMT1-100N and a load cell of 100 N were used. Operative speed was 0.5 mm min^{-1}. The distance between the support rollers (L) was set in 40 mm. Rectangular prisms with nominal dimensions of 4x4x45 mm were tested. Real values of width (w; mm) and thickness (t; mm) of each specimen resulted from the average of 3 measures throughout the sample. Flexural strength (σf; MPa) was calculated from maximum load (F; N) reached, according to the equation:

$$\sigma f = 3FL / 2wt2 \quad (2)$$

Reported flexural strength values for each material correspond to the mean of at least 11 tests.

Compressive strength (Su; MPa) and elastic modulus (E; MPa) were obtained from a test that consisting of applying a uniaxial compressive load on a specimen with known dimension, until its complete failure. An MTS Systems Corporation apparatus model SMT1-100N with a load cell of 5000N was used. Test conditions correspond to the standard ASTM C1424-15. Test specimens were cylinders with nominal diameter of 6.35 mm and 12.70 mm length. Real diameter used in the calculations corresponds to the average between 2 measures taken from each specimen.

The compressive strength calculations are based in the maximum load point before failure (Pmax; N) related to the specimen section (A; mm^2) according the next formula:

$Su=Pmax/A$ (3)

Elastic modulus E corresponds to the slope of the straight line in the elastic section in the representation of the stress (σ; MPa) versus deformation (ε) curve.

$E= \Delta\sigma/\Delta\varepsilon$ (4)

Ball milling abrasion tests were performed using 1 cm^3 cubic specimens. These cubes were subjected to a drum test adapted from ISO 556 standard, using a RETSCH MM400 ball mill device. The cubes were placed in a cylindrical stainless-steel drum of 55 mm length and 26 mm diameter (inner dimensions), containing a stainless-steel ball of 14 mm diameter. The drum was shaken at a frequency of 10 Hz for 60 s. Subsequently, the result was sieved over 0.5 mm, defining an abrasion index as the mass fraction (%) of fines with a particle size under ≤0.5 mm. Additionally, with comparative purposes, same index was measured in commercial cordierite cubes (Celcor® Corning Inc. 31 cells/cm^2) and the calcined epiphysis (400°C) of a sheep humerus.

3. – RESULTS AND DISCUSSION

As already mentioned, when the whey powder is deposited in a mold and heated to 150ºC, it takes place a pseudo-sintering process that gives rise to consistent pieces that retain the shape of the mold. This behavior is not due, as in the case of sugar (sucrose), to the melting and subsequent caramelization, since the whey does not go through a plastic or softening phase at any time. In order to understand the mechanism that gives rise to this pseudo-sintering, a TG/DTG thermogravimetric analysis was carried out on N_2 and CO_2 atmospheres, as described in the experimental section. The curves obtained in this analysis are shown in Fig. 3 (right).

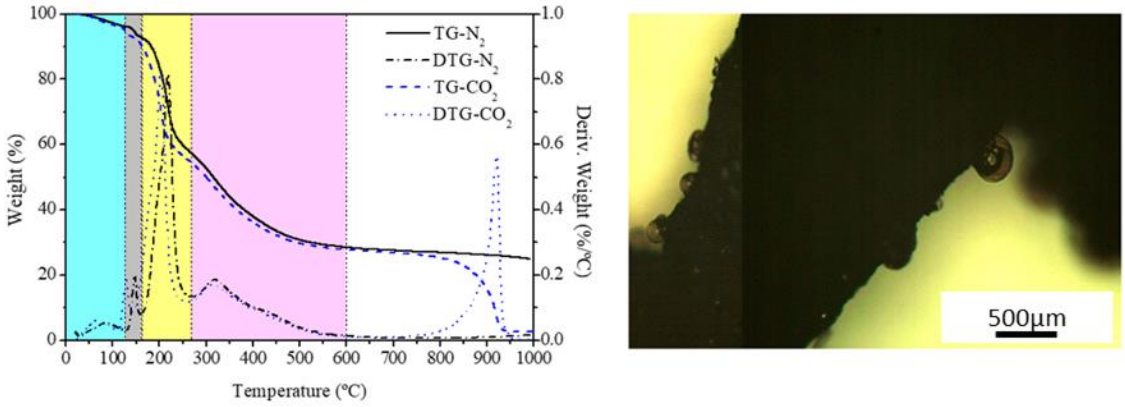

Fig. 3. TG/DTG curves of dehydrated whey powders (W) obtained in an atmosphere of N_2 and CO_2 (left).Droplets exuded at 200ºC observed with an optical microscope (right).

In short: between 130-160ºC, there is still release of water vapor and lactose begins to melt, impregnating the whey. From approximately 80 ºC and up to approximately 270ºC, the Maillard reaction occurs, the proteins react with the degradation products of lactose giving rise to a series of complex compounds that act as a glue that binds the whey particles [4]. A picture of the viscous droplets emanating from the whey surface at these temperatures can be seen in Fig. 3 (left). It is interesting to note that the chemical reactions that lead to caramelization, which in pure sugars would occur at about 235ºC; they occur at lower temperatures (120-150ºC) after the sugars have reacted with the amino acids [5]. Therefore, pseudo-sintering of the serum particles occurs at temperatures as low as 150 °C and without going through a melting state of the material. However, small droplets are produced that exude towards the surface of the particles that remain in a solid state. These drops, which solidify with temperature, could act as glue between the particles.

During the following stages of carbonization of the pieces already conformed, a release of volatiles occurs, which gives rise to the characteristic porosity of carbonized materials. At the same time, the walls that delimit the pores are reinforced. This produces porous but very consistent carbon materials.

In the case of activation, CO_2 begins to react with carbon at around 750ºC.

$C + CO_2 = 2CO$, Boudouard Reaction (4)

The maximum reactivity takes place around 900ºC (Fig. 3). After several activation tests were different temperatures were used, °C was found to be an optimal temperature at which micropore formation takes place homogeneously, since at 800 °C micropore formation is still insufficient and at 900 °C samples activate (burn) only at external zones, so micropore formation is also smaller.

From the above processes, porous carbon pieces can be obtained with very varied shapes, depending on the mold. Given the great consistency of these structures, they can also be machined to improve the finish of the pieces if necessary. In Figure 4 some examples of the type of structures that can be obtained are shown.

Two aspects to take into account when manufacturing porous carbon structures from whey powder are the yield and the shrinkage, with respect to the piece obtained at 150ºC, which takes place during carbonization or activation. The variation with carbonization or activation temperatures of yield in weight and shrinkage is shown in Fig. 5.

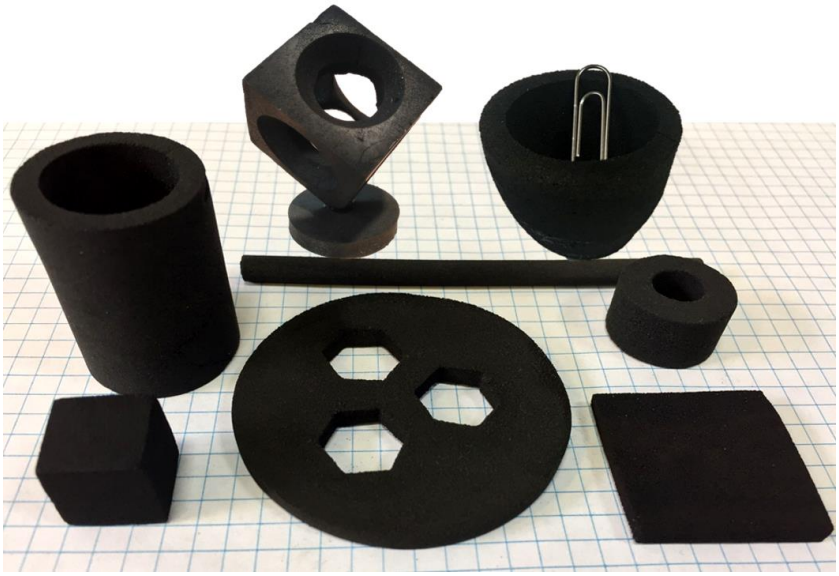

Fig. 4. Some of the porous carbon structures obtained by casting and machining.

As expected, yield decreases with carbonization temperature, being 26 wt% for the monoliths carbonized at 850 ºC (CW850). The activation of the material with CO_2 increases its porosity at the expense of the carbon consumed in the Boudouard reaction.

$C + CO_2 = 2CO$ (4)

Therefore, the yields of the activated materials are lower than for those carbonized. In the case of the pieces obtained by activation at 850ºC for 1.5 h (AW850/1.5), the yield is 18 wt% (Fig. 5).

ISSN-L: 0012-7361 | Vol. 96 nº4 | Jul-Aug 2021 | Dyna

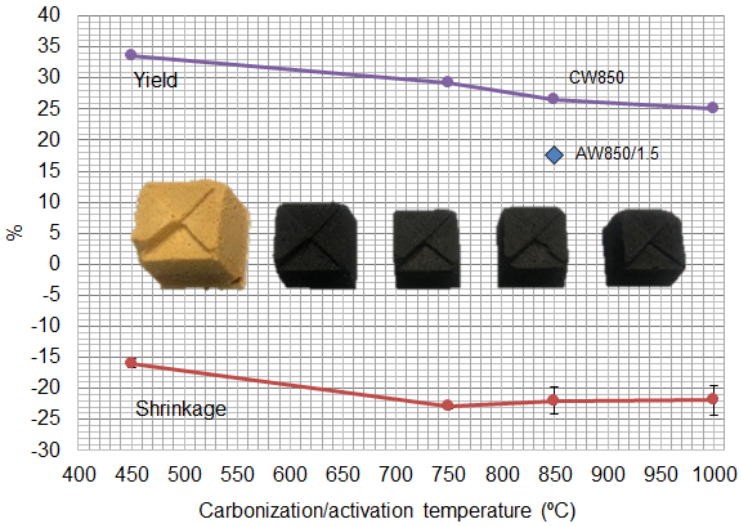

Fig. 5. Variation of the yield (wt%) and shrinkage of the porous carbon monoliths with the carbonization/activation temperature.

Regarding the shrinkage with respect to the piece extracted from the mold, which is a fact to take into account when designing a porous carbon structure obtained by this process, it has been validated that it is the same in the case of both carbonization and activation. This is possibly because the activation has been carried out once the piece has been carbonized. Therefore, it only influences the generation of microprosity in the walls that delimit the macropores, without reducing the total size of the piece. As can be seen in Fig. 5, the materials experience a significant shrinkage up to 750 °C, remaining practically constant at 23% shrinkage at higher temperatures. It is important to note that this contraction is linear and equal in any dimension (XYZ) of the structure, so the shape of the piece does not affect it.

The chemical properties of the carbons produced by sintering/carbonization of whey powder are summarized in Table 2.

Table 2. Chemical properties of the carbon monoliths.

Sample	Proximate Analysis (wt%)				Elemental Analysis[a] (wt%)					pH_{PZC}
	Moisture	Ashes	Volatile matter	Fixed Carbon	C	H	N	O	S	
CW850	12.2	6.1	12.5	69.2	68.0	1.2	2.3	13.4	0.2	11.1
AW850/1.5	13.7	18.1	5.6	62.5	64.5	0.8	3.0	14.0	0.2	11.3

[a]Dry basis

It is worth mentioning the relatively high ash content, which is due to the K, Ca and P content of the whey itself (Table 1). This mineral material, mainly phosphates and carbonates, can be removed, if necessary, relatively easily by washing with hot water or with acidified water for almost total elimination. On the other hand, the resulting carbons also have a relatively high N content with respect to other carbons, due to the fact that part of the N of the whey proteins remains in the structure of the carbons resulting from the treatment. This characteristic has been used to obtain other whey-derived carbons, although powdered and activated with KOH, which are suitable for the manufacture of electrodes for supercapacitors. [6].

The hierarchical porous structure is, together with being obtained by molding and machining, what characterizes these monolithic carbons obtained from whey. The term hierarchical porous structure refers to the fact that the pores presented by these materials are of very different sizes, so different techniques are needed to characterize them. For example, in Fig. 6, where photographs of carbonized materials (CW850) obtained by scanning electron microscopy (SEM) are presented, pores of up to 200 µm can be observed. These micrometric range macropores are characteristic of these materials and give them a great permeability.

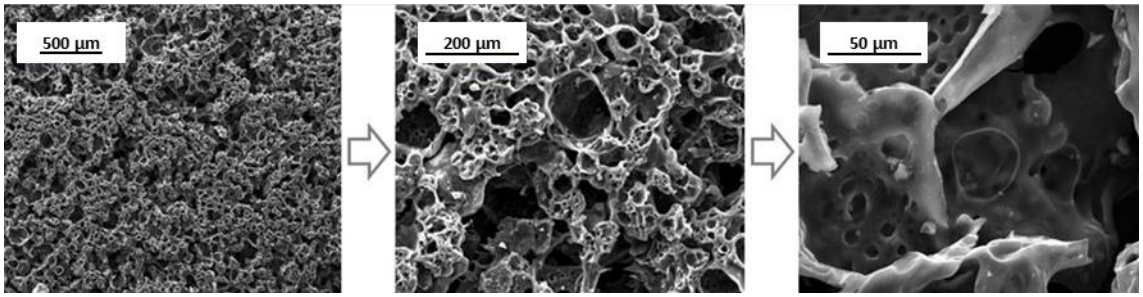

Fig. 6. SEM microphotographs of the porous carbon monoliths (CW850) at different magnifications.

Going down the scale, it can be observed, by Hg porosimetry (Fig. 7 right), that the macropores of these materials are around 23 µm for the carbonized material and 20 µm for the activated.

If we look at the material at even smaller scales, using N_2 adsorption isotherms at -196 ºC (Figure 7 left and Table 3) we can see that both materials present mesopores around 16.1 nm and 24.3 nm for CW850 and AW850/1.5 respectively and micropores around 1.2 nm. However, the activated material has, as expected, more than twice these micropores, its BET area being greater than 1000 m^2/g. Other materials carbonized at temperatures below 850ºC have hardly any micropores.

All this porosity, which as a whole is 58.7% for the carbonized material CW850 and 70.5% for the activated AW850/1.5, endows the porous carbon structures, obtained by sintering and subsequent carbonization or activation of the whey, with a high permeability, in particular to the gases. However, despite this high porosity, these materials have excellent mechanical properties as shown in Table 4.

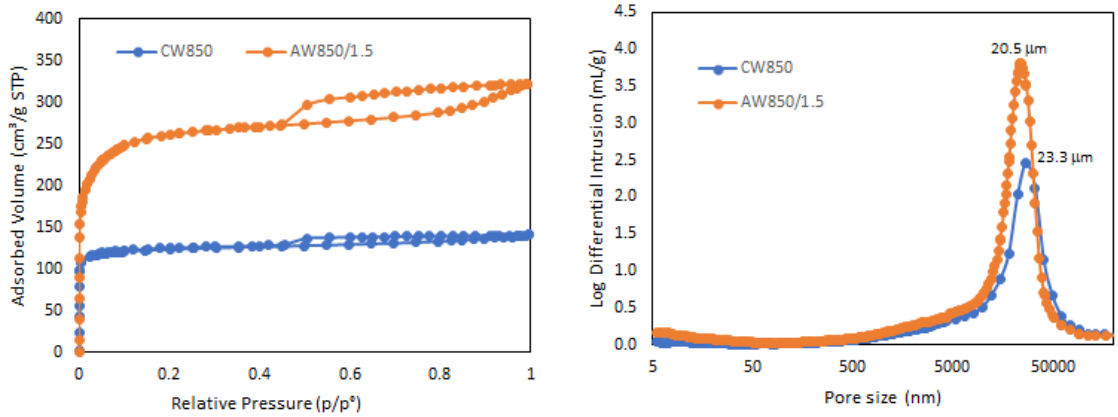

Fig.7. N_2 adsorption/desorption isotherms at -196 ºC (left) and pore size distribution obtained by Hg intrusion porosimetry (right).

Table 3. Main porous properties of carbon monoliths.

Sample	S_{BET} m^2/g	V_{DR} cm^3/g	V_{meso}[b] m^3/g	V_{total}[a] cm^3/g	d_{micro} nm	d_{meso} nm	ρ_{He} g/cm^3	ρ_{Hg} g/cm^3	P (%)
CW850	495	0.192	0.024	0.217	1.2	16.1	2.06	0.85	58.7
AW850/1.5	1017	0.431	0.066	0.497	1.2	24.3	2.10	0.62	70.5

[a]Calculated at $p/p^0 = 0.99$; [b]$V_{meso} = V_{total} - V_{DR}$.

ISSN-L: 0012-7361 | Vol. 96 nº4 | Jul-Aug 2021 | Dyna

Table 4. Permeability and mechanical properties of the carbon monoliths.

Muestra	Permeabilidad (k) m^2	Resistencia a la Flexión (f) MPa*	Resistencia a la Compresión MPa*	Módulo de Compresión GPa*	Índice de abrasión (% < 0.5 mm)*
CW850	4.9×10^{-12} (0.5 darcy)	14.3 ± 0.7	41.5 ± 5.7	1.3 ± 0,1	13.5 ± 1.3
AW850/1.5	4.2×10^{-12} (0.4 darcy)	7.5 ± 1.8	10.6 ± 4.3	0.8 ± 0.2	28.0 ± 5.1

The following comparisons allow contextualizing the values of the Table 4.

The permeability of a sand bed, depending on the size of the particles and the degree of compaction, is between 10^{-12} and 10^{-9} m^2 (1-1000 darcy) and the permeability of a porous carbon obtained from phenolic resins with particle sizes between 50 and 200 µm is between 3.5 and 14.5 × 10^{-12} m^2. These values, similar to those obtained in this work, are up to 10^4 times higher than those of porous carbon pellets produced by conventional pelletization. [7].

The flexural strength of porous carbons (40-50% porosity) obtained by 3D printing and commercializing as Carboprint® C by SGL Carbon is 5 MPa and its Young's modulus (compression) is 2 GPa. If these carbons are reinforced by infiltration into the pores of a polymer (Carboprint® P), the flexural strength and Young's modulus values increase to 45 MPa and 6 GPa respectively; but at the cost of losing porosity [8]. Comparing between porous carbons, those obtained in this work by molding and carbonization of powdered whey have a flexural strength of more than 3 times that of commercial porous coals, even having higher porosity (58.7%). While the activated carbons that have a porosity of 70.5% present a flexural strength greater than 7.5 MPa.

Regarding the compression strength, the structures obtained from carbonized whey reach values of 41.5 MPa, being 10.6 MPa in the case those activated. Porous carbon monoliths with similar characteristics to those presented in this work do not exceed 8 MPa [9-11]. Porous materials of carbon reinforced with alumina achieve values up to 9.1 MPa [12]. Other porous materials, with applications similar to those of whey-derived carbons, are adsorbent materials such as zeolites, with a compression strength of 5.2 MPa. [13]. In all cases, the carbons obtained from whey substantially improve the compression strength values. Other materials used in tissue engineering, such as hydroxyapatite or tricalcium phosphate (TCP), have compressive strength values of 34 MPa and 11 MPa respectively [14,15], while for human trabecular bone it is always lower than 15 MPa [14], all of them well below the compressive strength values achieved by the structures obtaining by carbonization of whey powder. This last comparison is made on the basis that one of the possible applications of these materials, given their characteristics, could be as scaffolds for tissue engineering, more specifically for bone regeneration. [16].

The abrasion index of a commercial cordierite (Celcor® Corning Inc. 31 cells/cm^2), used as catalyst support, is 20%, a value comparable to that of the activated monoliths obtained in this work and higher than that of the carbonized ones. On the other hand, the abrasion of the epiphysis calcined at 400ºC of a sheep humerus (87%) is much higher than that of the porous carbon structures obtained from whey.

Based on their characteristics, other possible applications for the whey-derived carbon structures could be:

Monoliths to remove contaminants [17]; monoliths and membranes for the separation of gases or compounds in liquid phase [18]; 3D electrodes for electrical energy storage systems [19]; custom 3D catalyst supports [20]; bioreactors, photocatalytic reactors and other multifunctional reactors [21].

4. – CONCLUSIONS

Heating dehydrated whey powder in a mold at 150 °C produces pieces of an organic porous material. These pieces, which already have a good consistency, can be transformed into porous carbon structures by carbonization or activation. The resulting porous carbons are characterized by the fact that they adopt the shape of the mold in which they are obtained, although with a slight isotropic shrinkage between 15% and 23%, depending on temperature of carbonization, and also because they have a hierarchical porosity, composed of macropores sized between hundreds of micrometers until 50 nanometers, mesopores and micropores that, as a whole, can be between 50% and 70%. This porosity gives them great permeability. However, they have very good mechanical properties, being more resistant to compression, bending and abrasion than many other materials with similar porosities, based on measurements made with international standards. This allows them to be machined with conventional tools, further expanding the possibilities of obtaining complex structures.

REFERENCES

[1] Menéndez JA, Martín-Gullón I. "Types of carbon adsorbents and their production" in Activated carbon surfaces in environmental remediation (Interface sci. and technol. series, 7. T. Bandosz Ed. ELSEVIER 2006 (ISBN: 0-12-370536-3) Ch. 1, 1-48. DOI: https://doi.org/10.1016/S1573-4285(06)80010-4

[2] Fortune Business Insights (2020) "Activated carbon market size, share & COVID19 impact analysis by type (powdered, granular and others), by application (water treatment, air & gas purification, food and beverage, others) and regional forecast, 2020-2027". Report ID: FBI102175. Recuperado de https://www.fortunebusinessinsights.com/activated-carbon-market-102175

[3] Baldasso C, Barros TC, et al. "Concentration and purification of whey proteins by ultrafiltration". Desalination. September 2011. Vol. 278. p. 381-386. DOI: https://doi.org/10.1016/j.desal.2011.05.055

[4] Cardoso JC, Albuquerque RLC et al. "Effect of the Maillard reaction on properties of casein and casein films" Journal of Thermal Analysis and Calorimetry. 2011. Vol.104 p. 249-254. DOI: https://doi.org/10.1007/s10973-010-1044-x

[5] Berg HE. "Reactions of lactose during heat treatment of milk: a quantitative study". Breg ed. 1993 (ISBN 90-5485-102-3). https://edepot.wur.nl/203007

[6] Tan S, Chen X et al. "Spray drying assisted synthesis of porous carbons from whey powders for capacitive energy storage". Energy. March 2018. Vol. 147. p. 08-316. DOI: https://doi.org/10.1016/j.energy.2018.01.066

[7] Tennison SR. "Phenolic-resin-derived activated carbons". Applied Catalysis A: General. October 1998. Vol. 173. p. 289-311. DOI: https://doi.org/10.1016/S0926-860X(98)00186-0

[8] URL: https://www.sglcarbon.com/en/markets-solutions/material/carboprint/

[9] Ibeh, P. O., et al. "Activated carbon monoliths from lignocellulosic biomass waste for electrochemical applications." Journal of the Taiwan Institute of Chemical Engineers 97. March 2019. p. 480-488. DOI; https://doi.org/10.1016/j.jtice.2019.02.019

[10] Taubert M. et al. "Attempts to design porous carbon monoliths using porous concrete as a template", Microporous and Mesoporous Materials, October 2014, vol. 197. P. 58-62. DOI; https://doi.org/10.1016/j.micromeso.2014.06.005

[11] Szczurek A, Fierro V et al, Emulsion-templated porous carbon monoliths derived from tannins, Carbon, August 2014,vol. 74, p. 352-362, DOI; https://doi.org/10.1016/j.carbon.2014.03.047

[12] Zhong Y et al. "Synthesis of a novel porous material comprising carbon/alumina composite aerogels monoliths with high compressive strength", Microporous and Mesoporous Materials, May 2013, vol. 172, p. 182-189, DOI; https://doi.org/10.1016/j.micromeso.2013.01.021

[13] Wang S, Bai P et al. "Fabricating Mechanically Robust Binder-Free Structured Zeolites by 3D Printing Coupled with Zeolite Soldering: A Superior Configuration for CO2 Capture", Advanced Science, Septembre 2019, vol. 6, art. 1901317, DOI; https://doi.org/10.1002/advs.201901317

[14] Woodard J, Hilldore A, et al. "The mechanical properties and osteoconductivity of hydroxyapatite bone scaffolds with multi-scale porosity", Biomaterials, January 2007, vol. 28, Is. 1, p. 45-54, DOI; https://doi.org/10.1016/j.biomaterials.2006.08.021

[15] Bose S, Roy M, and Bandyopadhyay A. "Recent advances in bone tissue engineering scaffolds." Trends in biotechnology, October 2012, vol. 30, n.10, p. 546-554, DOI; https://doi.org/10.1016/j.tibtech.2012.07.005

[16] Yan Y, Chen H, et al. "Vascularized 3D printed scaffolds for promoting bone regeneration". Biomaterials, January 2019. Vol. 190-191. p. 97-110 DOI: https://doi.org/10.1016/j.biomaterials.2018.10.033

[17] Monash University (2018) URL: https://www.monash.edu/__data/assets/pdf_file/0009/1463778/Carbon-monoliths-water-purification.pdf

[18] Bara JE, Hawkins CI, et al. Nanomaterials and Energy. "3D printing for CO2 capture and chemical engineering design" September 2013. Vol 5. p. 235-243 DOI: https://doi.org/10.1680/nme/13.00021

[19] Fu k, Yao Y, et al. "Progress in 3D Printing of Carbon Materials for Energy-Related Applications" Advanced Materials. March 2017. Vol. 29. p. 1603486. DOI: https://doi.org/10.1002/adma.201603486

[20] Parra-Cabrera C, Achille C. et al. "3D printing in chemical engineering and catalytic technology: structured catalysts, mixers and reactors". Chemical Society Reviews. January 2018. vol. 40. p. 201-230. DOI; https://doi.org/10.1039/C7CS00631D

[21] Konarovla DM, Aslam W, et al. "Enabling Process Intensification by 3 D Printing of Catalytic Structures". ChemCatChem. November 2017. Vol- 9. p. 4132-4138 DOI: https://doi.org/10.1002/cctc.201700829

ACKNOWLEDGMENTS

The authors are grateful for the support of the Principado de Asturias-FICYT-FEDER (Project PCTI-Asturias IDI/2018/000118) and MINECO (Project CTQ2017-87820-R). We thank Massimiliano Forlano (CAPSA FOOD) for the whey powder samples and Dr. Gregorio Marbán for his help in measuring the He permeabilities.

SUPPLEMENTARY MATERIAL

A video on the fabrication and machining of whey-derived porous carbon structures is available at this link: https://youtu.be/HOrUZam7QRE